Int J Adv Manuf Technol (2013) 69:245–256
DOI 10.1007/s00170-013-5025-7

ORIGINAL ARTICLE

CO_2 laser butt-welding of steel sandwich sheet composites

Konstantinos Salonitis · Panagiotis Stavropoulos · Apostolos Fysikopoulos · George Chryssolouris

Received: 11 January 2013 / Accepted: 19 April 2013 / Published online: 9 May 2013

Abstract Steel sandwich sheets compared with conventional steel exhibit significant performance improvements such as lower density, higher specific flexural stiffness, and better sound and vibration damping characteristics. However, the main challenge for the broad industrial use is that the joining and assembling methods be used in such a way so as not to alter significantly these characteristics. In the present paper, a laser welding of steel sandwich is examined. The feasibility study of the laser butt-welding of sandwich steel sheets with a CO_2 laser beam has revealed that such an approach is possible. A theoretical model of the laser welding process is developed for the investigation of the laser beam impact on both the core and the outer steel layers of the sandwich material. The model presented is based on a novel idea for the simulation of the heat source through the finite element analysis for the estimation of the temperature distribution. Additionally, the effect on the quality of the weld, the strength of the welded sheet, and its damping characteristics are also experimentally investigated and prove that laser welding can be considered as an alternative joining process.

Keywords Laser welding · Steel composites · Modeling · Finite element analysis

K. Salonitis · P. Stavropoulos · A. Fysikopoulos · G. Chryssolouris (✉)
Laboratory for Manufacturing Systems and Automation, Department of Mechanical Engineering and Aeronautics, University of Patras, Patras 265 00, Greece
e-mail: gchrys@hol.gr

G. Chryssolouris
e-mail: xrisol@lms.mech.upatras.gr

K. Salonitis
Manufacturing and Materials Department, School of Applied Sciences, Cranfield University, Bedford MK43 0AL, UK

Nomenclature

A	Material absorptivity
C_p	Specific heat
H	Enthalpy
h	Free convection film coefficient
h_k	Keyhole depth
k	Thermal conductivity
L	Characteristic length of the surface
L_m	Equivalent latent heat of melting
L_v	Equivalent latent heat of vaporization
Nu	Nusselt number
Pe	Peclet number
P_L	Laser beam power
q_0	Maximum laser intensity of the beam
Q_{conv}	Heat transfer due to convection
Q_{rad}	Heat transfer due to radiation
Q_{sur}	Heat transfer at the surface due to laser irradiation
Q_{vol}	Volumetric heat generation rate
r	Radial coordinates
r_k	Keyhole radius
r_0	Laser beam radius at the workpiece surface
T	Temperature
T_v	Equivalent vaporization temperature
T_o	Initial temperature
u_w	Welding speed
x, y, z	Cartesian coordinates

Greek symbols

ε	Heat emissivity
ζ	Distance from focal plane
σ	Stefan–Boltzmann constant
ρ	Material density

Subscripts

i=1, 2	Material type (1 for metal layers, 2 for viscoelastic core material)
j=A, B, C	Sheet layer type (A the upper metallic blank, B the viscoelastic core, and C the lower metallic blank)

1 Introduction

The transportation industry is continuously looking for lighter materials to improve product efficiency; thus, the use of composites is becoming more prevalent throughout the automotive, aerospace, and railway sectors. Polymer–polymer composites are often used, but despite being lightweight, they have the disadvantage of limited formability after the initial part creation, and are generally formed into the final shape during the initial molding. Sandwich steel composites have been recently introduced and consist of stiff outer layers, connected by a relatively low-density core, exhibiting high specific strength and stiffness that may lead to substantial design advantages. They are thought as being a considerable versatile option for the replacement of a full metal construction since they can be formed like metals, but offer weight savings, approaching those of polymer composites. The use of such materials in the automotive industry for specific applications (indicatively in the floor and dash panels for attenuating specific frequencies) can reduce the need for a number of additional processes (e.g., the need of adhesives for achieving noise and vibration damping). However, the main limitation in the use of sandwich steel composites is that they should be mechanically fastened or adhesively bonded. In many cases, the overlap joints are not desirable as they lead to stress concentrations, thick sections, and reduced weight savings. Welding could create viable butt joints, eliminating the problems arising from the overlap joints. The constituent properties of the sandwich composites are greatly influenced by the temperature and moisture fields. For example, extreme temperature changes, such as those created during the laser welding process as well as the humid environmental conditions, can significantly degrade the stiffness and strength of the viscoelastic core. Previous studies [1] have proposed a finite element model for the simulation of the laser welding of sandwich materials. Two different approaches were investigated; either through the performance of the welding of the sandwich material on both sides, in a controlled way, in order for overheating of the viscoelastic core to be avoided or through the application of the conventional one side welding for the joining of the two sandwich sheets. The former approach was found to be feasible for such joining and revealed that the upper and lower steel sheets could be welded up to 70 % by causing less than 10 % damage to the core material. The one side approach, however, was proven ineffective to weld the sheets and prevent any damage from being caused to the core material in the vicinity of the weld. Gower et al. [2] have identified that laser spot welds on sandwich materials are very susceptible to cracking due to high cooling rates that cause large stresses. These high cooling rates are necessary in order to prevent the excessive thermal degradation of the central polymer layer. They address a technique to provide such high cooling rates, while preventing cracking in AA5182 thin sheet during pulsed laser welding. The ramped down pulse shape limited the crack length, indicating that pulse shaping may be effective; however, the power of the pulsed laser used was too high to provide sufficient control over the final cooling stage.

Few published studies are available about the laser welding of such composite materials. Due to the different composition of materials, the laser welding of sandwich materials falls into the greater field of laser welding of dissimilar materials. Dissimilar metal joints are characterized by compositional gradients and micro-structural changes that produce large variations in physical and chemical properties across the joint. Potential problems include those associated with joining the component materials individually, and those being specific to the different compositions and properties of the base materials in various proportions. Weld quality depends on the characteristics of the laser beam, the particular processing parameters, and the physical and chemical properties of the base metals. The addition of a filler material introduces additional variables such as feed parameters, widening the range of potential weld-metal composition. The principal physical properties of the base materials that influence laser welding are thermal conductivity, absorptivity, density, specific heat capacity, thermal expansion coefficient, and melting temperature.

Numerous studies report on the laser welding of various grades of stainless steels. The influence of the laser beam position, with respect to the joint on weld characteristics, has been investigated by Berretta et al. [3] using a pulsed Nd:YAG laser source to weld AISI 304 with AISI 420 stainless steels. Tensile tests indicated that fracture occurred outside the weld regions, showing that the weld region had a higher tensile strength than had the base metals. Mousavi et al. [4] studied the weldability of AISI 321 and AISI 630 stainless steels, focusing on the effect of laser power, beam diameter, and pulse duration on the width and depth of the welds. Results indicated that both weld depth and width increased while the laser power was increased, but varied bilaterally with the pulse duration. Anawa et al. [5] utilizing the Taguchi method have targeted the optimization of welding parameters in minimizing the fusion zone. The case study has been performed on AISI 316, stainless steel, and AISI 1009 low carbon steel plates utilizing a CO_2 continuous laser source. Variable parameters of the study included laser power, welding speed, and focus width, and the conclusion was that the welding speed is the key factor for the consideration of the fusing area size.

Apart from the studies made on laser welding of mild steel with stainless steel, a large number of investigations have been published about the weldability of steel with other materials as well. Laser welding of tool steel and Kovar [6] reveal a sizeable intermixing of the individual constituents in the weld region. There was no hot cracking of the joint observed, while cross sections of the weld seam exhibited strong convection currents. The porosity observed in the weld seam had a seemingly visible relationship with the welding speed.

Increase in the welding speed resulted in a decrease in the number of pores, while their average size was increased. The welding of steel with other materials, using filler wires, has also been investigated in [7], while the welding of AISI 310 austenitic stainless steel with nickel based alloy Inconel 657 required four types of filler materials. The results revealed that welding with Inconel A filler wire presented the least hot cracking sensitivity, and the weld region had the highest strength and elongation properties.

The behavior of dissimilar metal welding between steels and various superalloys has also been investigated. Autogenous full penetration welding of Ni-based superalloy K418 and alloy steel 42CrMo 3.5 mm thick flat plates were conducted using a 3-kW CW Nd:YAG laser by Liu et al. [8]. Their main result was that although the micro-hardness of the weld seam was lower than that of the base metals, the joint was as strong as the base metal. Pandremenos et al. [9] examined experimentally CO_2 laser welding of dissimilar grades of Advanced High Strength Steels, specifically the joining of PM/CP800 and PM/CP1000. Through a statistical analysis, the effect of each parameter on the geometrical characteristics was estimated. The welding speed had the greatest impact, and the gas pressure was the least important process parameter.

In this paper, the use of CO_2 lasers for the welding of sandwich steels, as a means of delivering tailored blanks, is investigated both theoretically and experimentally. A heat source model is presented, and it is based on the idea of a combined source, having resulted from the surface irradiation of the workpiece, due to laser beam and a volumetric source due to the keyhole gases. A finite element model is developed for the investigation of the heat impact on both the core and the outer steel layers of the sandwich material. The feasibility of the CO_2 laser welding process is experimentally investigated. The effect of the laser welding process on the quality of the weld, the strength of the welded sheet, and its damping characteristics are also experimentally investigated. The main outcome of the present study is that there is evidence that laser welding can be considered as an alternative joining process. Future work will focus on the selection of the process parameters' optimization and the derivation of confident process window maps.

2 Laser welding of sandwich material

2.1 The challenges

Laser welding of sandwich materials with a viscoelastic core is limited due to its heat-sensitive core. The core is usually composed of resin with a relatively low melting point (300 to 500 °C). Laser welding should occur in such a way so as to avoid seriously affecting and damaging the viscoelastic core. The goal is that the welding caused deterioration of the damping and acoustical properties of the material be minimized. Salonitis et al. [1] investigated theoretically two different approaches (one- and two-sided welding) of the laser welding of sandwich material in an attempt to minimize the impact of the process on the core (Fig. 1).

The one-sided welding approach will result in the evaporation of some of the viscoelastic core. Thus, controlling the amount of the core material to be sacrificed is significant. The two-sided approach is based on the welding of the sheets on both sides. The main challenge is to control the depth of the welding through proper selection of process parameters, without having the temperature of the core raised above its melting temperature. The theoretical study has indicated that this is possible but lacks in experimental verification. Besides the selection of the process parameters, the type of laser source to be used is also important. The Nd:YAG laser wavelength is better absorbed by most of the materials (copper, aluminum, precious metals, etc.). Steel, however, exhibits acceptable absorption levels when irradiated by CO_2 lasers beams. Furthermore, the CO_2 laser sources can achieve higher powers at a lower cost. The CO_2 laser processing is an established solution for various machining processes such as drilling, cutting, and grooving [10–12]. The use of CO_2 lasers for welding is not common, and only few studies have been presented [9]. However, from an industrial point of view, such a possibility would be desirable. Park et al. [13] have used CO_2 laser welding to describe the mechanism of the plasma and spatter, as it varied by welding conditions such as welding speed and laser power, and the resulting change in the bead shape of galvanized steel.

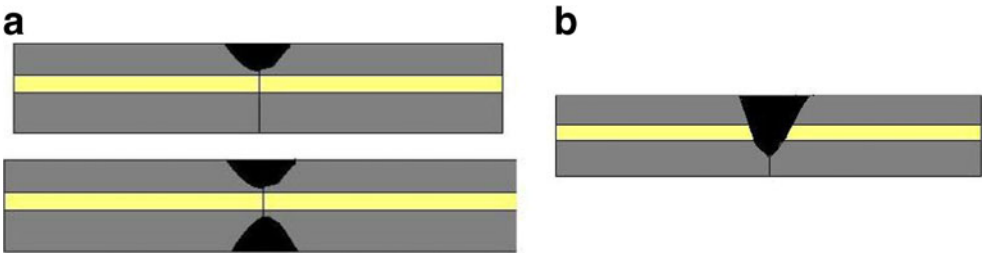

Fig. 1 Laser welding of sandwich materials **a** two-sided approach, **b** one-sided approach [1]

2.2 Feasibility study

The welding of commercially available sandwich steel was experimentally investigated with the use of a CO_2 laser system. The sandwich laminate comprised two 0.55-mm steel sheets of IF260 with a yield stress of 260–320 MPa separated by a viscoelastic polymer core (45 μm). Furthermore, the outer surfaces of the steel blanks were coated with HDG+Z140. The CO_2 laser system operated in a pulsed mode with 10 KHz frequency, at 7.5 in. focal length and a beam radius at 0.25-mm focal point. The focal plane was positioned at 1 mm above the blank surface. An air knife was used for delivering N_2 shielding gas at 8 bars. The experimental setup and a sample feasibility part are shown in Fig. 2.

A number of single-sided experiments were designed and implemented revealing that through welding of the blanks can be achieved. All experiments were repeated five times. Preliminary visual inspection of the specimens indicated that there are a number of process parameters combinations that can result in through welds. Table 1 summarizes the experimental design and the outcome of the visual inspection. The main outcome of this investigation was that through welds can be achieved, but the process parameters have to be controlled otherwise the process might result in either burning significant amount of the core material or in forming dross in the lower blank requiring subsequent post-processing.

Table 1 Feasibility experiments outcome

		Laser power (W)				
		800	1,000	1,200	1,400	1,600
Welding speed (cm/min)	60	PWP	Good	ED	ED, ECB	ECB
	80	NT	Good	Good	ED	ECB
	100	NT	PWP	Good	Good	ECB
	120	NT	NT	Good	Good	Good
	140	NT	NT	NT	PWP	ECB

NT not through weld, *PWP* poor weld profile, *ECB* excessive core burn, *ED* excessive dross formation

3 Theoretical analysis

During laser welding, only a small portion of the energy transferred by the laser beam is absorbed by the workpiece material, due to the material's emissivity [14]. The energy absorbed initially causes a local temperature rise at the material's surface, and soon, the vicinity of the laser spot reaches melting temperature which results in the formation of a molten pool. The high energy density further increases the temperature which reaches that of vaporization. The pressure of the vapor gases results in the formation of a "keyhole," sustained during the laser welding procedure that follows the laser beam. The keyhole laser welding process can be thus simulated by two heat sources, a surface one, accounting for the laser beam delivery of energy, and a volumetric one for taking into consideration the keyhole gases. Furthermore, the volumetric heat source accounts for the effects of the laser light's multiple reflections on the keyhole walls and further resulting in an increase of the laser intensity towards the lower end of the keyhole. However, a portion of the energy is lost due to the convection between the workpiece material and the surrounding environment. The use of assisting gas (either for protecting the laser head mirror or for confining the plasma plume generation) further increases the convection coefficient.

As the mechanical properties of the weld are highly dependent on the cooling rate of the weld of the metal,

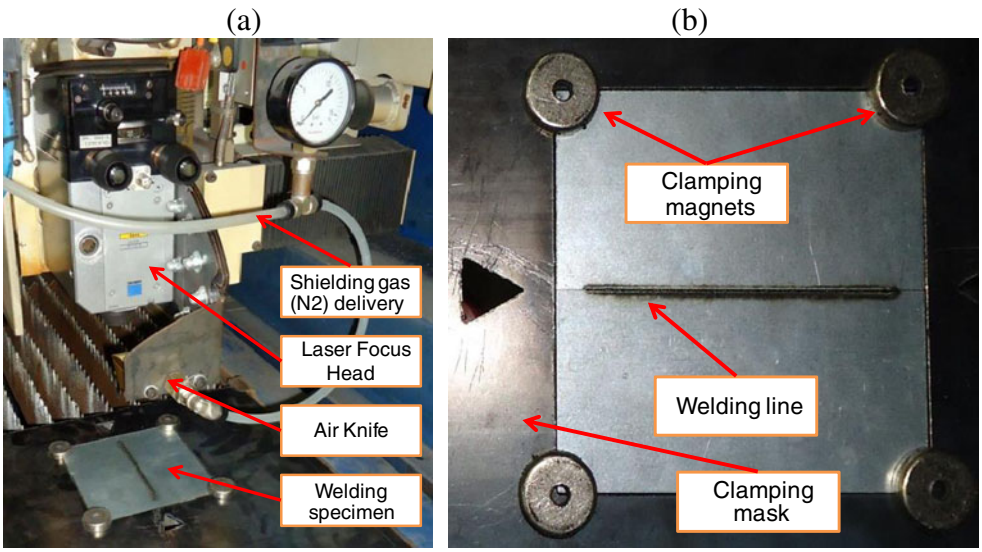

Fig. 2 Laser welding of steel sandwich sheet **a** experimental setup and **b** feasibility part as clamped for welding (P= 1,550 W and u_w=80 cm/min)

having knowledge of the temperature field in and around the molten pool is essential for the modeling of the welding process. Many models were proposed for laser welding that would predict the temperature distributions being of great importance for in-depth analysis and eventually the improvement of the process.

The process can be considered as a transient heat conduction problem. The differential equation, governing the heat conduction within the workpiece, is

$$k_i(T_j)\left\{\left(\frac{\partial^2 T_j}{\partial x^2}\right)+\left(\frac{\partial^2 T_j}{\partial y^2}\right)+\left(\frac{\partial^2 T_j}{\partial z^2}\right)\right\} + Q_{\text{vol}} = \rho_i(T_j)\cdot C_{p,i}(T_j)\cdot\frac{\partial T_j}{\partial t} \quad (1)$$

Where x, y, z are the Cartesian coordinates, Q_{vol} is the volumetric heat generation rate, ρ is the material density, k is the thermal conductivity and C_p is the specific heat. All thermal properties of the material are considered being functions of the temperature T, for i denoting the material type (i=1 for the metal layers and i=2 for the viscoelastic core material) and j denoting the sheet layer (j=A the upper metallic blank, j=B the viscoelastic core and j=C the lower metallic blank).

The boundary conditions are defined by the surface heat source, the heat convention and radiation at the upper surface of the workpiece, the surface convention between the mating surfaces of the viscoelastic material and the metal blanks and finally, the surface convention at the lower surface, as it can be seen in Fig. 3.

Having considered the various heat exchanges, the boundary for the upper surface (z=0) can be defined as:

$$-k_1(T_A)\left.\frac{\partial T_A}{\partial z}\right|_{z=0} = -Q_{\text{sur}}(r)\cdot \text{for}\, r \le r_0 \quad (2)$$

$$-k_1(T_A)\left.\frac{\partial T_A}{\partial z}\right|_{z=0} = Q_{\text{conv}}(T_A)\cdot \text{for}\, r > r_0 \quad (3)$$

$$-k_1(T_A)\left.\frac{\partial T_A}{\partial z}\right|_{z=0} = Q_{\text{rad}}(T_A)\cdot \text{for}\, \mathrm{r} \le \mathrm{r}_0 \quad (4)$$

where, r_0 is the laser beam's radius at the workpiece surface. Equation 2 accounts for the heat entering the workpiece due to the surface heat source (Q_{sur}). Equation 3 accounts for the heat lost due to the free convection (Q_{conv}) at the upper surface, and Eq. 4 accounts for the heat loss due to the thermal radiation (Q_{rad}) between the weld and the environment.

In the interface between the metallic sheets and the viscoelastic core, the heat flow is being modelled using the Fourier law that results in the following two conditions:

$$-k_1(T_A)\left.\frac{\partial T_A}{\partial z}\right|_{Z=Z1} = -k_2(T_B)\left.\frac{\partial T_B}{\partial z}\right|_{Z=Z1}\cdot \text{for}\, \mathrm{z} = \mathrm{z}_1 \quad (5)$$

$$-k_2(T_B)\left.\frac{\partial T_B}{\partial z}\right|_{Z=Z2} = -k_1(T_C)\left.\frac{\partial T_C}{\partial z}\right|_{Z=Z2}\cdot \text{for}\, \mathrm{z} = \mathrm{z}_2 \quad (6)$$

Finally, at the lower surface, heat lost due to convection, with the boundary condition defined as:

$$-k_1(T_C)\left.\frac{\partial T_C}{\partial z}\right|_{Z=Z3} = Q_{\text{conv}}(T_C) \quad (7)$$

3.1 Heat input

The heat input required for the formation of the weld is provided by the laser beam energy. As already mentioned, it is well documented that the heat input can be modelled more accurately by considering a surface and a volumetric heat source. The surface heat source was estimated based on the analytical equation provided by Tsoukantas et al. [15]

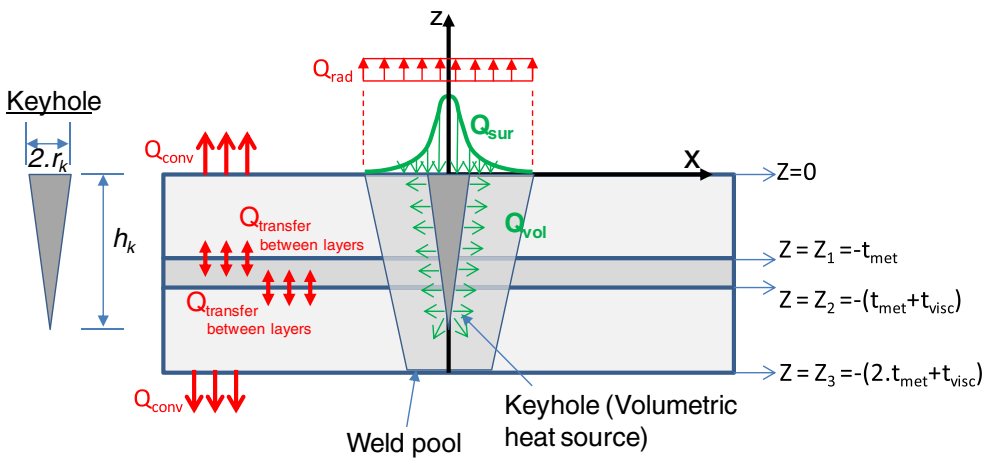

Fig. 3 Simulation "envelope" and boundary conditions (with t_i being the thickness of each sheet)

considering that the laser beam presents a Gaussian intensity distribution:

$$Q_{\text{sur}}(r) = A \cdot q_0 \cdot \exp\left(-\frac{2r^2}{r_0^2}\right) \tag{8}$$

where $Q_{\text{sur}}(r)$ is the heat input intensity distribution of the beam on a circular laser beam spot, r is the position length of an arbitrary point within a laser beam's spot with respect to the centre of the spot, A is the material's absorptivity, r_0 is the laser beam radius at the workpiece surface, and q_0 is the maximum laser intensity of the beam on a circular laser beam spot that can be determined as a function of the power (P_{L}) of the laser beam as of:

$$q_0 = \frac{P_{\text{L}}}{r_0^2 \pi} \tag{9}$$

A number of researchers [16, 17] have simulated the volumetric heat source in keyhole laser welding as being of conic geometry. In the present study, the authors compared the results of a conic heat source versus a cylindrical one that was used in their previous attempt of simulating the process [1], and found that the conical heat source simulated the process with higher accuracy.

The dimensions of the conic heat source need to be estimated on the basis of the existing literature. For the needs of the present study, the depth of the heat source was estimated based on the work presented by Tsoukantas and Chryssolouris [18] due to the fact that closed form equations were provided as a function of the equivalent thermo-physical properties of the materials:

$$h_{\text{k}} = \frac{AP_L}{\log(1.5)\pi r_0 \rho u_{\text{w}} \left[C_{p,eq}(T_{\text{v}} - T_0) + L_{\text{m}} + L_{\text{v}}\right]} \tag{10}$$

Where h_{k} is the keyhole depth, u_{w} is the welding speed, T_{v} and T_{o} is the equivalent vaporization temperature and the initial temperature, respectively, and L_{m} and L_{v} are the equivalent latent heat of melting and vaporization.

On the other hand, the keyhole's radius is estimated using the following equation as derived by Moraitis and Labeas [19]:

$$r_{\text{k}} = \frac{k}{\rho C_p} \frac{2\text{Pe}}{u_{\text{w}}} \tag{11}$$

Where Pe is the Peclet number that can be estimated approximately based on Moraitis and Labeas [19] and Solana and Ocana [20] analysis.

Therefore, the volumetric heat load (Q_{vol}) due to a conical shaped heat source with radius r_{k} and depth h_{k} can be determined by the following equation, derived on the basis of Moraitis and Labeas's work [19]:

$$Q_{\text{vol}}(r,\zeta) = \frac{2P_{\text{L}}}{\pi r_{\text{k}}^2 h_{\text{k}}} \left(1 - \frac{\zeta}{h_{\text{k}}}\right) \exp\left(1 - \left(\frac{r}{r_{\text{k}}}\right)^2\right) \tag{12}$$

where, ζ is the distance from the focal plane along the laser beam propagation.

3.2 Heat loss due to convection

The energy that is lost due to convection at the upper and lower surfaces is due to free convection, following thus Newton's law:

$$Q_{\text{conv}}(T) = \frac{k\text{Nu}}{L}(T - T_0) = h(T - T_0) \tag{13}$$

Where Nu is the Nusselt number, L is the characteristic length of the surface, and h the free convection film coefficient. The average Nusselt numbers can be estimated for each surface of the workpiece using the relations stated by the authors in [1] as a function of ambient air properties and temperature differences between the surface and the environment. Subsequently, the average values of the convection film coefficients can be calculated.

3.3 Heat loss due to radiation

Significant radiation losses on the model's external surfaces can occur only when the temperature difference between the heated surface and the environment is high. For this reason, they are considered being negligible for all the surfaces besides the welded area. In this area, such heat losses can be estimated using the Stefan–Boltzmann relation:

$$Q_{\text{rad}}(T) = \varepsilon\sigma\left(T^4 - T_0^4\right) \tag{14}$$

Where ε is the heat emissivity and σ is the Stefan–Boltzmann constant.

The heat loss, due to radiation from the bottom surface, is considered negligible since the keyhole depth is always less than the thickness of the sandwich sheet. Therefore, the bottom surface temperature is always less than the vapor temperature thus, justifying the neglect of heat radiation. However, in order to prove this assumption, solving the simulation for the case of maximum keyhole depth with the thermal radiation of the bottom sheet considered has resulted in a 2.6 % change of the temperature estimation. Nevertheless, the finite element model required twice as much of the initial time for its solution.

3.4 Finite element model development

The aforementioned heat transfer analysis made it clear that it would be practically impossible for the system of equations to be analytically solved. For this reason, a Finite Element Analysis (FEA) model was developed using the ANSYS commercial code, based on a previous study presented by Salonitis et al. [1].

A large number of papers investigating the laser welding processes of monolithic materials have been published; however, the study of the relevant literature has revealed the lack of simple models capable of describing the laser welding process of sandwich steel composite materials, such as the ones considered in the present study. Over the last years, the theoretical papers have been focusing on the simulation of the process with the use of the finite element analysis. The outcome of these works can also be adapted to the simulation of the sandwich materials. Mazumder and Steen [21] developed one of the first numerical models of the continuous laser welding process. This model implemented the finite difference technique for a Gaussian beam intensity distribution assuming a constant absorption coefficient. Goldak et al. [22] introduced a double ellipsoidal type of representation of the welding arc in the context of fusion arc welding and also showed its suitability for modeling high penetration welding. Frewin and Scott [23] proposed a 3D FEA model for pulsed laser welding. Through experiments, they found the heat flux distribution to be conical. The measured longitudinal power density distribution within the beam, as a function of distance from the focused spot, revealed the influence of the position of the focal point on the final weld bead dimensions. Maiti et al. [24] studied the heat transfer following the double ellipsoidal representation of the laser beam, which also incorporated a volumetric heat source. The temperature dependence of material properties, phase change phenomena, and convective and radiation heat losses from all the surfaces of a sheet were considered. Shanmugam et al. [25] developed a FE model for high power density welding process in order to estimate the shape of the weld beads for different ranges of laser input parameters. The temperature profiles computed using a Gaussian heat source delivered the temperature distribution only on the top surface of the sheet and not along the thickness direction. Abderrazak et al. [26] developed a model for the determination of the penetration depth and the bead width as a function of both incident laser power and welding speed of magnesium alloys. The proposed model was based on the Davis thermal approach for the estimation of the capillary diameter. A FE model was also developed in [27] for controlling the penetration depth and width of the molten material, contributing to the thickness control of the intermetallic compound layer, in laser welding of the magnesium alloy AZ31B and aluminum alloy A5052-O. It was revealed that the edge-line welding lap joint could realize the shallow penetration depth of molten metal into lower plate, which would be effective for reducing the reaction between two metals and then the formation of intermetallic compound. Finally, Shanmugan et al. [28] investigated the transient temperature profiles of a laser weld joint utilizing a 3D FE model, in aim of obtaining the temperature field behavior and molten pool shape during the process.

For the needs of the present study, the mesh of the geometry was developed in such a way so as to be finer in the area of the weld seam and to further allow the application of localised volume heat sources (corresponding to the keyhole cavity; Fig. 4). Furthermore, since the blanks to be virtually welded were composites made of two steel sheets mated together with a viscoelastic core, two different material models were used, one for the top and bottom steel layers and one for the viscoelastic core lying in between. Eight quadrilateral node elements were chosen for the meshing of the geometry, with singular degree of freedom being the temperature that could however compensate for the mass transport heat flow from a constant velocity field.

The heat transfer between the adjacent materials was modelled using a contact target parameter. The contact target parameter was set through virtual elements that overlaid the solid ones at the mating surfaces. Contact occurs when the element surface penetrates one of the target segment elements on a specified target surface. In the present paper, a contact surface is the bottom surface of the upper metal sheet of the sandwich material, whereas a target surface is the upper surface of the material's core. Similarly, a contact surface exists between the bottom surface of the core and the upper surface of the lower metal sheet. In order for the analysis time to be reduced and more accurate results to be achieved, only half of the model used had its symmetry exploited.

The accuracy of the FEA predictions was determined by the way the model was actually loaded (geometric characteristics and magnitude of the loading conditions) and the simulation of the heat transfer mechanisms from the workpiece to the environment (through the proper selection of heat transfer coefficients). For the determination of the heat transfer coefficients to and from the environment, analytical relationships from literature were used as per Salonitis et al. [9]. Temperature-dependent thermal material properties, as shown in Fig. 5, were used for the base material. The

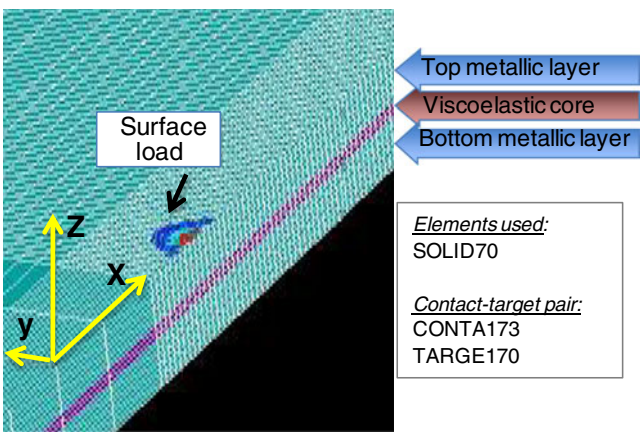

Fig. 4 Finite element model meshing and loading

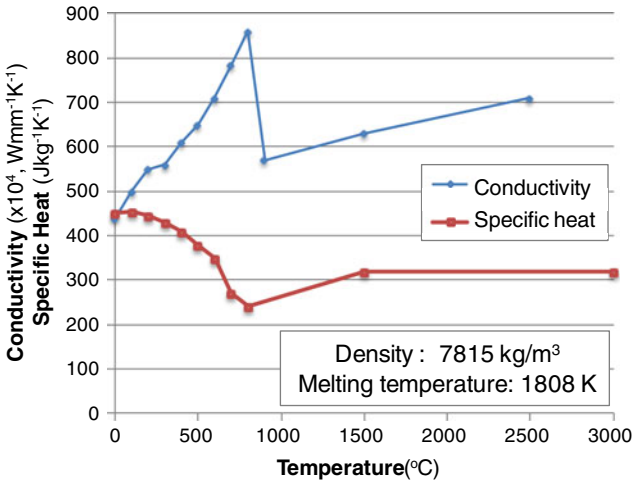

Fig. 5 Material properties used in FE simulation as per [29] for the case of metallic upper and lower blanks

mechanical properties of the metallic blanks are also presented in Fig. 5. A lack of information on the properties of the viscoelastic material resulted in the use of average values (Table 2) independent of the temperature as per [1].

The mesh size was determined through a sensitivity analysis. Meshes containing different number of elements were generated (each subsequent mesh had twice the number of elements of the previous one). The acceptance criterion was for two subsequent meshes to present less than 2 % average difference in the calculated temperature profiles. The final meshing resulted in approximately 12,000 elements. The model developed was verified in the case of 3-mm-thick butt-welding stainless steel sheets through the comparison of experimental results [1].

3.5 Theoretical results

The feasibility study pointed out the difficulties of the two-sided welding approach, even in a laboratory environment. Practical difficulties such as handling large size blanks, the need for rigid large size fixtures, and the precise alignment of the laser beam would limit industrialization. Therefore, the theoretical model developed was solved only for the one-sided approach so as to define the process parameters window that would allow for the minimum impact on the viscoelastic core.

The criteria for the successful welding are the welding depth and the width of weld pool. In the case of sandwich steel composites welding, another significant parameter can be considered being the amount of viscoelastic core burned. This characteristic can be quantified through the void size that is being generated when the core material is burnt during the process. These characteristics can all be estimated by the temperature distribution, calculated with FEA as it can be seen in Fig. 6.

The fluctuations of the void size, triggered by alternation in the welding speed and the laser power, were investigated. The theoretical results, at a constant welding speed, have shown that the void increases as the laser power does so. However, once the welding takes place at the lower steel sheet, as the laser power is being increased, the void tends to reach a constant size of approximately 0.6 mm that physically equals two times the heat-affected zone (HAZ) of the steel material, at the vicinity of the core (Fig. 7).

Simulations at a constant laser power and a variable welding speed (Fig. 8) have shown that welding through the sandwich material is possible without further deteriorating the core. Low welding speeds (in the range of 40–80 cm/min) indicate that the size of the void again reaches a stable value. Once the core has been burnt, there are no means of heat conduction. Increasing the welding speed above 80 cm/min results in decreasing the void and consequently, in maintaining the viscoelastic core's properties in the welded sub-product. The results indicate that both the welding speed and the laser power are crucial parameters for the quality of the welding. Another interesting finding is that the increase in the laser beam's diameter results in reduced welding depths. This result can be physically justified since an increase in the beam's diameter results in reduced power density values and thus, in more heat being dissipated closer to the surface of the workpiece rather being used for the maintenance of the volumetric heat source, which is responsible for the welding depth.

Table 2 Core material properties [1]

Property	Symbol	Value
Density	ρ	1,320 kg/m^3
Specific heat	c_ρ	2,300 J/kg.K
Enthalpy	H	50 J/kg
Thermal conductivity	K	0.5 W/m.K
Melting temperature	$T_{m,2}$	450 °C

4 Experimental investigations

4.1 Microstructural analysis

For the assessment of the weld quality, the welding parameters were selected on the basis of the theoretical results. The experiments were conducted with the setup described in Section 2.2. The specimens were welded, cut, polished, and then etched with 4 % picarl and 2 % nital etchants for the visualization of the welding area and the HAZ. The microscopy inspection has revealed that a number of enclosures and pores are formed within the weld (Fig. 9a). It is believed

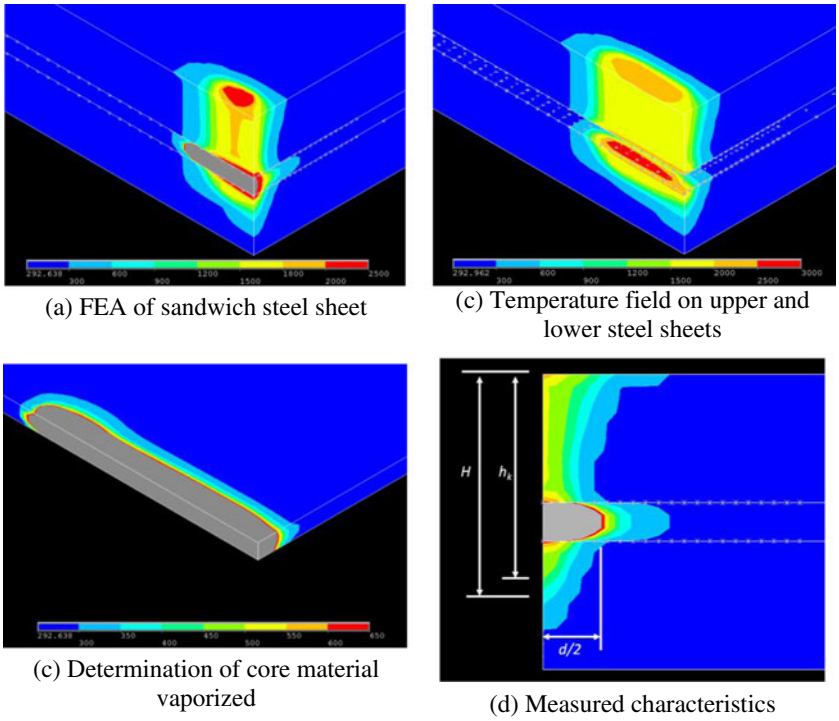

(a) FEA of sandwich steel sheet

(c) Temperature field on upper and lower steel sheets

(c) Determination of core material vaporized

(d) Measured characteristics

Fig. 6 FEA of the laser welding of sandwich steel for estimating core material deterioration (size of void–d/2) and welding depth (H). Results for P=2,000 W and u_w=80 cm/min

that the underlying cause for these pores is the entrapment of gas within the solidified weld. The gas is the result of the viscoelastic core vaporization. Since the exact chemical composition of the viscoelastic core is not known, it cannot be safely predicted whether enough hydrogen is generated due to vaporization that could lead to hydrogen embrittlement. In most cases, the pore geometry was elongated and appeared to be having a tail. This is justifiable due to the fact that gas attempted to escape while the metal was still in a liquid state (known as wormhole porosity). Such enclosures can result in local strain concentrations, formulating cracks that might cause early failure of the weld. Additionally, such entrapments can be caused by the vaporization of the steel's upper and lower coating layers.

A possible solution to eliminating such pores could be through the "cleaning" of the vicinity of the weld by preheating. The welding line is laser scanned with low power, in order for the temperature to be increased above the coating and the core's melting temperature, without however causing metal melting. Afterwards, welding can take place. Experiments resulted in pore-free welds through this approach (Fig. 9b). However, this solution resulted in increased overall processing time. Alternatively, the bespoke development of a laser system through the incorporation of two laser beams in order for these two process steps to be combined into one could be promising. However, in the case of an industrial environment, using two laser beams and subsequently two laser sources would highly increase the fixed costs. Another approach would be the integration of a beam splitter into the beam delivery system, in order to first pre-heat and then laser weld. On the other hand, such a sequential process can be used only for straight

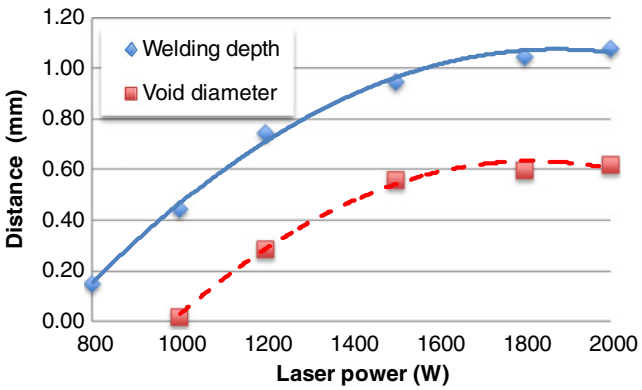

Fig. 7 Laser power effect on welding depth and void size (u_w=80 cm/min)

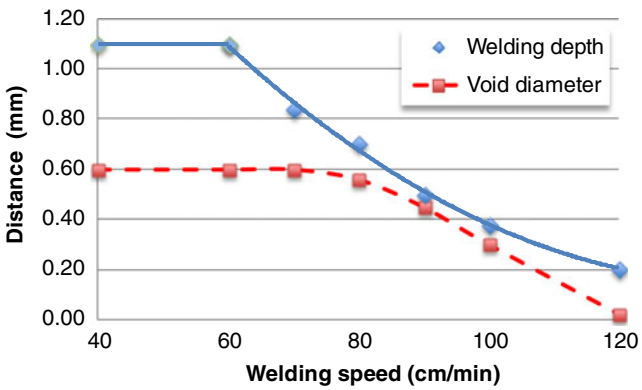

Fig. 8 Scanning speed effect on welding depth and void size (P_L= 1,300 W)

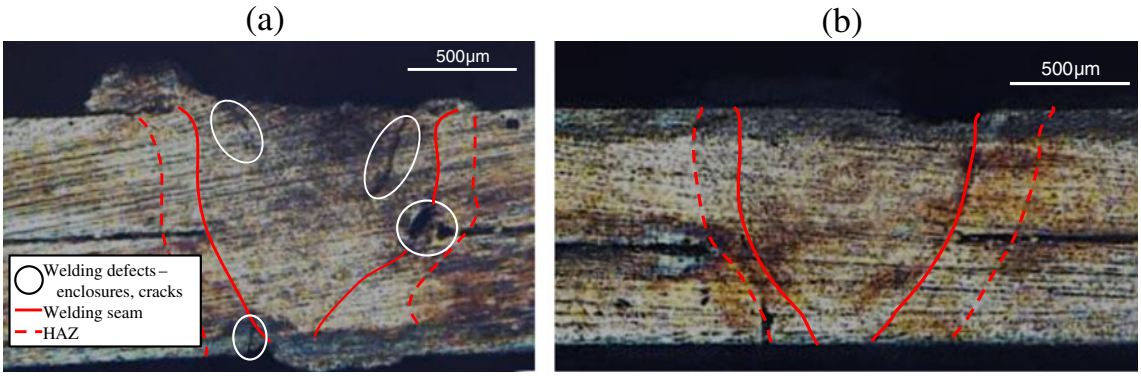

Fig. 9 Laser welding of steel tests **a** without and **b** with preheating (P_L=1,800 W and u_w=100 cm/min)

welds. This kind of approach could be possibly implemented at a lower cost, requiring though a thorough investigation so as to become mature enough to be industrially applicable.

4.2 Mechanical tests

The welded blanks need to retain the mechanical properties of the initial blanks. However, welding leads to the formation of a soft zone in the subcritical area of the HAZ and the mechanical properties of the welded joints are affected by this area. It is important that the engineers understand the mechanical behavior of laser-welding seams. Past investigations in non-composite steel blanks have revealed that their weldability is significantly dependent on their chemical composition and the various coating that might exist. As an example, the ferrite/austenite balance has a remarkable influence on both the mechanical and corrosion properties of stainless steels and significantly influences the laser weldability of these materials [30]. The current industrial trends focus on the reduction of carbon content and attain the strength by alloying elements and/or thermal processing during rolling. These fine-grained steels are particularly suitable for the low-heat-input laser welding process in order for the development of a coarse-grained microstructure in the HAZ region to be avoided. Previous investigations have demonstrated that the micro-structure of both weld and heat-affected zones is a function of the cooling rate from peak temperature [31, 32].

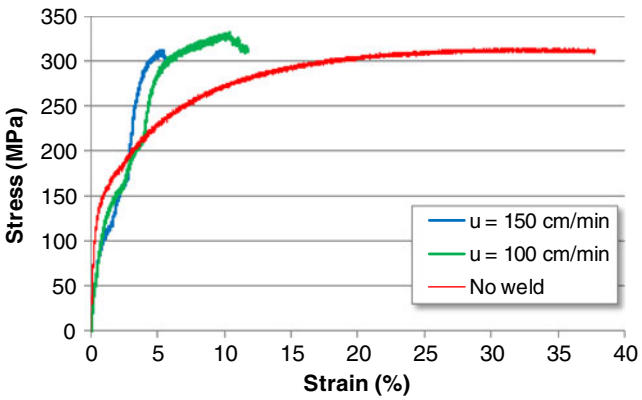

Fig. 10 Tensile strength test results for welded specimens with a CO_2 laser (P=1,800 W and pulsing frequency f=10,000 Hz)

In the present study, the mechanical properties of the weld were assessed through tensile strength tests. The thermal cycles associated with laser beam welding are generally much faster than those involved in conventional arc welding processes, leading to a rather small weld zone. Thus, it is rather difficult for the tensile properties of a laser weld joint area to be determined due to the small size of the fusion zone. Complete information on the tensile and fracture toughness properties of the fusion zone is essential for prequalification and a complete understanding of the joint performance in service, as well as for the conduction of the defect assessment procedure of such dissimilar weld joints.

The main result was that the ultimate strength of the material was not affected by the process parameters selected and the weld exhibited tensile strength close to that of the base material (Fig. 10). However, the failure behavior changed from ductile to brittle. The failure took place close to the weld, but not on the weld itself. This could be possibly attributed to the residual stresses caused by the temperature rise during the welding process. Furthermore, the temperature rise led to the formation of soft zones with hardness near the weld profile being significantly lower than that of the rest of the blank. This soft zone took place up to a distance of 1/2 HAZ in either side, a result that was in agreement with Cam et al. [33].

4.3 Damping tests

The damping properties of the composite material were assessed through the Frequency Response Function (FRF) measurements. The FRF is capable of isolating the inherent dynamic properties of a mechanical structure. Three identical parts (automotive floor panels) formed by steel, steel composite, and tailored welded steel composite were

measured after excitation, with the use of accelerometers in various positions. Figure 11 indicates that the steel composite structure presents the best damping characteristics, whereas the tailor welded composite steel still exhibits far better attenuation properties than those of the monolithic steel floor part. Rapid temperature changes, such as those created during the laser welding process as well as the humid environmental conditions, degrade the stiffness and strength of the viscoelastic core, resulting in reduced Noise, Vibration, and Harshness (NVH) performance when compared to non-welded steel composites. As it was theoretically indicated [1], retaining of the composite's NVH performance can be achieved if less than 10 % of the core material is sacrificed during the welding. Furthermore, as investigated in [2], during welding, high cooling rates necessary for the prevention of the core layer's excessive thermal degradation cause large stresses that further result in cracking within sandwich materials. However, micro cracks result in reduced damping characteristics and hence lower NVH performance [2].

5 Conclusions

The butt laser welding of steel composite blanks was investigated. The effect of the process parameters on the welding geometry was theoretically assessed. A heat source model was developed that accounted for both the surface irradiation of the workpiece, due to the laser beam and the heat generated and transferred to the workpiece due to the keyhole gases. The temperature distribution was estimated through a finite element model. The theoretical results indicated process parameter combinations that could lead to through welds with less damaged viscoelastic core. The subsequent experimental feasibility tests revealed that such a model could be used for the offline control of the process; however, further experimentation is required for fine-tuning the model and for increasing confidence.

The effect of the welding on the strength and the damping characteristics of the blank was also presented. The former was investigated through typical tensile strength tests. The comparison of welded specimens with those of a base material has shown that the ultimate strength of the material was not affected by the process parameters and that the weld exhibited tensile strength close to that of the base material. However, its failure behavior changed from ductile to brittle. The damping tests proved that the tailor-welded composite steel exhibited far better attenuation properties than those of the monolithic steel floor part.

It can be stated that there is enough evidence to prove that the production of tailor-welded blanks from steel composites is feasible. This kind of blanks can substitute the conventional ones in vehicle applications where increased damping is required, for the improvement of the NVH performance, without the cost and the processing needs being increased. Future work will focus on the selection of the process parameters' optimization and the derivation of confident process window maps.

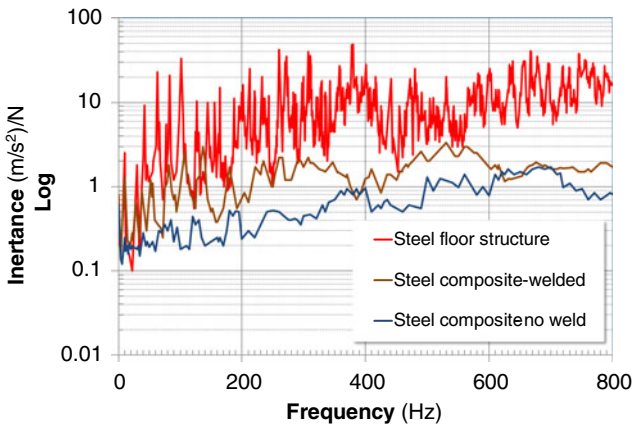

Fig. 11 Noise, Vibration and Harshness (NVH) comparison of a steel, steel composite, and tailor-welded blank steel composite

Acknowledgments The work reported in this paper was partially supported by CEC/FP6 NMP Programme, "Integration Multi-functional materials and related production technologies integrated into the Automotive industry of the future-FUTURA" (FP6-2004-NMP-NI-4-026621).

References

1. Salonitis K, Drougkas D, Chryssolouris G (2010) Finite element modeling of penetration laser welding of sandwich materials. Phys Procedia 5:327–335. doi:10.1016/j.phpro.2010.08.059
2. Gower HL, Pieters RRGM, Richardson IM (2006) Pulsed laser welding of metal-polymer sandwich materials using pulse shaping. J Laser Appl 18:35–41. doi:10.2351/1.2080307
3. Berretta JR, de Rossi W, das Neves MDM, de Almeida IA, Vieira ND Jr (2007) Pulsed Nd:YAG laser welding of AISI 304 to AISI 420 stainless steels. Opt Lasers Eng 45:960–966
4. Mousavi SAA, Akbari, Sufizadeh AR (2009) Metallurgical investigations of pulsed Nd:YAG laser welding of AISI 321 and AISI 630 stainless steels. Mater Des 30:3150–3157
5. Anawa EM, Olabi AG (2008) Using Taguchi method to optimize welding pool of dissimilar laser-welded components. Opt Laser Technol 40:379–388
6. Mai TA, Spowage AC (2004) Characterization of dissimilar joints in laser welding of steel–kovar, copper–steel and copper–aluminium. Mater Sci Eng, A 374:224–233
7. Naffakh H, Shamanian M, Ashrafizadeh F (2009) Dissimilar welding of AISI 310 austenitic stainless steel to nickel-based alloy Inconel 657. J Mater Process Technol 209:3628–3639
8. Liu X-B, Yu G, Pang M, Fan J-W, Wang H-H, Zheng C-Y (2007) Dissimilar autogenous full penetration welding of superalloy K418 and 42CrMo steel by a high power CW Nd:YAG laser. Appl Surf Sci 253:7281–7289
9. Pandremenos J, Salonits K, Chryssolouris G (2009), «CO_2 Laser Welding of AHSS», Proceedings of the ICALEO 2009—28th

International Congress on Applications of Lasers and Electro-optics, 2–5 November, Orlando, FL, USA, (Paper P122), pp. 1507–1514, ISBN: 978-0-912035-59-8
10. Salonitis K, Stournaras A, Tsoukantas G, Stavropoulos P, Chryssolouris G (2007) A theoretical and experimental investigation on limitations of pulsed laser drilling. J Mater Process Technol 183:96–103. doi:10.1016/j.jmatprotec.2006.09.031
11. Stournaras A, Stavropoulos P, Salonitis K, Chryssolouris G (2009) An investigation of quality in CO_2 laser cutting of aluminum. CIRP J Manuf Sci Technol 2:61–69. doi:10.1016/j.cirpj.2009.08.005
12. Stournaras A, Salonitis K, Stavropoulos P, Chyssolouris G (2009) Theoretical and experimental investigation of pulsed laser grooving process. Int J Adv Manuf Technol 44:114–124. doi:10.1007/s00170-008-1818-5
13. Park H, Rhee S (1999) Analysis of mechanism of plasma and spatter in CO_2 laser welding of galvanized steel. Opt Laser Technol 31:119–126
14. Chryssolouris G (1991) Laser machining: theory and practice. Springer, New York
15. Tsoukantas G, Salonitis K, Stournaras A, Stavropoulos P, Chryssolouris G (2007) On optimal design limitations of generalized two-mirror remote beam delivery laser systems: the case of remote welding. Int J Adv Manuf Technol 32:932–941
16. Lankalapalli KN, Tu JF, Gartner M (1996) A model for estimating penetration depth of laser welding processes. Phys D: Appl Phys 29:1831–1841
17. Lampa C, Kaplan AFH, Powell J, Magnusson C (1997) An analytical thermodynamic model of laser welding. Phys D: Appl Phys 30:1293–1299
18. Tsoukantas G, Chryssolouris G (2006) Theoretical and experimental analysis of the remote welding process on thin lap-joined AISI 304 sheets. Int J Adv Manuf Technol 35:880–894
19. Moraitis GA, Labeas GN (2008) Residual stress and distortion calculation of laser beam welding for aluminum lap joints. J Mater Process Tech 198:260–269
20. Solana P, Ocana JL (1997) A mathematical model for penetration laser welding as a free-boundary problem. J Phys D: Appl Phys 30:1300–1313
21. Mazumder J, Steen WM (1980) Heat transfer model for cw laser material processing. J Appl Phys 51:941–947
22. Goldak J, Chakravarti A, Bibby M (1984) A new finite element model for welding heat sources. Metall Trans B 15B:299–305
23. Frewin MR, Scott DA (1999) Finite element model of pulsed laser welding. Welding Research Supplement 5s–22s
24. Maiti SK, De A, Walsh CA, Bhadeshia HKDH (2003) Finite element simulation of laser spot welding. Sci Technol Weld Join 8:377–383
25. Siva SN, Buvanashekaran G, Sankaranarayanasamy K (2012) Some studies on weld bead geometries for laser spot welding process using finite element analysis. Mater Des 34:412–426
26. Abderrazak K, Salem WB, Mhiri H, Lepalec G, Autric M (2008) Modelling of CO2 laser welding of magnesium alloys. Opt Laser Technol 40:581–588
27. Borrisutthekul R, Miyashita Y, Mutoh Y (2005) Dissimilar material laser welding between magnesium alloy AZ31B and aluminium alloy A5052-O. Sci Technol Adv Mater 6:199–204
28. Siva Shanmugam N, Buvanashekaran G, Sankaranarayanasamy K, Manonmani K (2009) Some studies on temperature profiles in AISI 304 stainless steel sheet during laser beam welding using FE simulation. Int J Adv Manuf Technol 43:78–94
29. Martinson P, Daneshpour S, Kocak M, Riekehr S, Staron P (2009) Residual stress analysis of laser spot welding of steel sheets. Mater Des 30:3351–3359
30. Tavares SM, Terra VF, Pardal JM, Fonseca MP (2005) Influence of the microstructure on the toughness of a duplex stainless steel UNS S31803. J Mater Sci 40:145–154
31. Jana S (1992) Effect of heat input on HAZ properties of two duplex stainless steels. J Mater Process Technol 33:247–261. doi:10.1016/0924-0136(92)90211-A
32. Bala SP, Muthupandi V, Dietzel W, Sivan V (2006) Microstructure and corrosion behavior of shielded metal arc welded dissimilar joints comprising duplex stainless steel and low alloy steel. Mater Eng Perform 15:758. doi:10.1361/105994906X150902
33. Çam G, Erim S, Yeni Ç, Koçak M (1999) Determination of mechanical and fracture properties of laser beam welded steel joints. Weld Res, Weld Res Suppl 1999:193–201